MINISTRY OF EDUCATION AND TRAINING
QUY NHON UNIVERSITY

TRUONG DUY HUONG

SYNTHESIS OF MS_2 (M = Mo, W) AND THEIR MODIFICATION WITH g-C_3N_4 AS PHOTOCATALYSTS

Major: Physical and Theoretical Chemistry
Code No.: 9440119

SUMMARY OF DOCTORAL THESIS IN CHEMISTRY

BINH DINH - 2021

This work has been completed at:
Quy Nhon University and KU Leuven

The Board of Supervisors: **Assoc. Prof. VO VIEN**

Reviewer 1: **Dr. Nguyen Van Thang**

Reviewer 2: **Assoc. Prof. Nguyen Duc Cuong**

Reviewer 3: **Assoc. Prof. Tran Thi Van Thi**

The thesis shall be defended by University Examination Board at Quy Nhon University, An Duong Vuong Str. 170, Quy Nhon city, Binh Dinh province at ……../…. ...…../ 2021

The thesis can be found at:

- Library of Quy Nhon University
- Vietnam National Library

BINH DINH - 2021

INTRODUCTION

1. Problem statement

Along with the development of many areas of industries the arising of environmental pollution has become more and more serious. A lot of hazardous chemicals have been released into water and air, resulting in severe consequences for human health, such as dyes from textile industry, antibiotics from aquaculture, pesticides and herbicides from agriculture, etc., that urgently requires effective methods to solve the problem. Heterogeneous photocatalyst, which is one of advanced oxidation processes, has attracted attention of many scientists due to its ability to treat wastewater containing organic pollutants just using light with suitable wavelength and air oxygen as oxidant source. One of the most photocatalysts that has been used widely is TiO_2 owing to its low-cost, chemical stability and nontoxicity. However, the big drawback of this catalyst comes from its UV light absorption. To find a solution for this, a variety of techniques can be applied, including modifying TiO_2 and the other oxide photocatalysts by doping with metal and non-metal elements, decorating with photosentitizers, etc., to make them become activated in the visible range of light. Another way has also been studied broadly is fabrication of photocatalysts which themselves working in the region of wavelength ranging from 400-600 nm. MoS_2 and WS_2, two members of the transition metal dichalcogenide family, possess the corresponding bandgaps of 1.3 eV and 1.35 eV, indicating that both of them can be excited by the visible light. As similar to the other photocatalysts, using separately could lead to an unavoidable phenomenon, namely high rate of recombination of photoinduced

electron and hole. Thus, apart from searching an effective method of synthesis, the finding of way of slowing down the recombination rate is also an important task. From this high demand of production of such photocatalysts to meet the practical amount the following topic was chosen as my PhD thesis, "*Synthesis of MS_2 (M = Mo, W) and their modification with g-C_3N_4 as photocatalysts*".

2. Objective of the thesis

This thesis aims to find a facile method of synthesis and evaluation of MS_2 (M = Mo, W) and the composites MS_2/g-C_3N_4 as visible-light-driven photocatalysts and building a system that can transfer them from lab scale into practical application.

3. Scope of the thesis

- The object of this thesis: the evaluation of photocatalytic activity of synthesized MS_2 (M = Mo, W) and their modified forms, as well as designing a pilot that can employ the materials for wastewater treatment.

- The scope of the thesis: The method used for the synthesis involving the solid state reaction and the modification of MS_2 (M = Mo, W) carried out by combining them with g-C_3N_4. The evaluation of photocatalytic activity mainly based on the degradation of dyes, including rhodamine B and methylen blue, the photodecomposition of an antibiotic enrofloxacin also explored using the better catalyst. The building of photocatalytic pilot for using the prepared materials just focused on a simple method of recovering the used catalyst involving the natural sedimentation and automating the system.

4. Significances

This thesis not only has significances in science, but also in practical is as follows:

- Scientific significance: Building synthesis processes of both MS_2 (M = Mo, W) and the composite MS_2/g-C_3N_4 using solid state reaction, the investigating the photocatalytic activity the obtained materials indicated the importance of adsorption in the whole photocatalysis process, the more the amount of organic pollutant adsorbs onto the photocatalyst, the larger the efficiency of photodegradation of that target molecule the catalyst exhibits. Nevertheless, the so high adsorption could lead to a negative effect on the whole process. Apart from low power, the monochromatic light emitted from light emitted diode could result in a high photochemical space-time yield compared to the others such as incandescent and xenon lamps.

- Practical significance: Simplifying the photocatalyst synthesis process of the visible-light driven materials, this resulted in a large amount of the catalysts that meets the real requirements. Designing the pilot, which can be a flexible and practical approach, in other word, that design could be a part of a complete wastewater treatment system or used separately and the light could be changed from an artificial source of low power to sunlight depending on the situation.

5. Thesis contributions

This thesis provides 04 main contributions as follows:

- Successful synthesis of both MS_2 (M = Mo, W) and the composite MS_2/g-C_3N_4 from sodium molybdate dihydrate and tungstic acid as molybdenum and tungsten sources, respectively and thiourea as a source of sulfur. The prepared processes were not only facile but

also resulted in a large amount of the materials that would meet the demand of using photocatalyst in practical application.

- The adsorption-photocatalysis relation to the whole photocatalytic process was clarified through the study of pH effect on the photocatalytic activity of the prepared materials. This might be meaningful for the choosing of suitable photocatalyst for a particular target to reach the highest efficiency.

- Light emitted diode (LED) became the best option lamp compared to the others in terms of the efficiency of using electricity, a crucial element in real application using a new benchmark, namely photochemical space-time yield (PSTY).

- A simple design for a photocatalytic pilot that meets the basic requirements of using photocatalyst for water treatment polluted by organic substances such as maximizing the contact between the catalyst and the wastewater, continuously mixing with air to ensure the dissolved oxygen enough for the photodegradation, using LED of low power, etc. Furthermore, in order to be practically feasible the designed pilot can be operated automatically and easily connected to the complete system in which the pilot is just one of the modules.

Chapter 1. LITERATURE REVIEW

The first photocatalyst studied in 1972 by Fujishima and Honda is TiO_2 acting as an anode for water spliting in a photochemical cell . So far, TiO_2 has become the most widely investigated photocatalyst due to its unique photocatalytic efficiency, photo-stability, low cost, nontoxicity, availability, thermal and chemical stability. Besides TiO_2 and the other photocatalyst ZnO have exhibited their advanced photocatalytic activity for wastewater treatment as well. However, they all possess the same disadvantage that they do not work under the visible light because of their large band gap, *e.g.* anatase form of TiO_2 has the band gap of 3.2 eV, which significantly prevent them from using solar energy for activation. This is due to the fact that in the solar spectrum ultraviolet light acounts for only 4-5%, meanwhile the visible light makes up to nearly 40% of the solar energy. To dealt with this vital deficiency, a lot of effort has been made to develop the novel materials which themselves active under the visible light without any modification.

MoS_2 and WS_2 are materials that belong to a family of transition metal chalcogenides (TMDs) with layered structure in which each unit (MS_2) comprises a transition metal (M = Mo, W) layer sandwiched between two sulfur atomic layers. As bulk form MoS_2 (2H) is an indirect bandgap semiconductor with a bandgap value of 1.3 eV, when reducing the sample thickness down to a few atomic layers or even to a 2H monolayer the bandgap is widened to 2.1 eV. Similarly, the bandgap of WS_2 has the value of 1.35 eV for bulk material as indirect and approximate 2.0 eV for monolayer as direct one. This optical

property suggests that such materials can strongly absorb in the visible region of the solar spectrum, and it is more appropriate when using as a cocatalyst.

Similar to the other photocatalysts such as TiO_2, MS_2 (M = Mo, W) has been widely used in the form of composites to improve the photocatalytic activities of the individual components, especially in the field of photocatalysis on photodegradation of organic contaminants. Among various partners that MS_2 (M = Mo, W) combine with, g-C_3N_4 has been considered as a promising candidate due to its electronic structure with band gap of 2.7 eV, in addition to low-cost, abundance of source, non-toxicity and chemical stability. The combination of MS_2 and g-C_3N_4 to create a composite is favourable, therefore, a facile method to synthesize a large amount of the materials compared to the previous reports without compromising photocatalytic activity is still in need. The overview also suggests that the study of adsorption role during the photocatalytic process need to be taken into account in the photocatalytic activity evaluation. Besides, the suitable choice of light source for the photocatalysis that could lead to a highly efficient reaction system with a high photochemical space-time yield, a new benchmark for photocatalytic reactors comparison. In order to bring the photocatalyst from to the practical application, a wide variety of reactors have been studied. However, a simple design which can be applied automatically in the real situation is still required.

Chapter 2. EXPERIMENTAL SECTION

2.1. Chemicals and equipments

The chemicals and equipments used in this thesis are listed here.

2.2. Material fabrications

- Fabrication of WS_2/g-C_3N_4
- Fabrication of MoS_2/g-C_3N_4

2.3. Characterizations

- Material characterizations

For characterization of the samples, powder X-ray diffraction (XRD), transmission electron microscope (TEM), scanning electron microscope (SEM) images were recorded by JEOL JSM-600F equipped with an energy dispersion X-ray spectrum (EDS). Infrared and Raman spectra were recorded using IRAffinity-IS (Shimadzu) spectrometer and Raman spectra were using T64000 Raman with a 647.1 nm laser as an excitation source and detector CCD was cooled by liquid nitrogen, respectively. The thermogravimetric-differential scanning calorimetry analysis was carried out on the SETRAM LABSYS TG system under air or argon flow with heating rate of 10 ^oC/min. The optical properties were examined on a Jasco V-650 Spectrophotometer (No. UV-1800) using $BaSO_4$ as reference. The surface area of samples were determined with TriStar 3000 V6.07 A. X-ray photoelectron spectroscopic (XPS) measurements were made on an Escalab 250Xi system.

- Determining point of zero charge
- Light spectra and intensity

2.4. Photocatalysis experiments

- Reaction system,
- Photocatalytic activity evaluation procedure,
- Standard curve construction,
- Measurement of emitted irradiance using spectrophotometer probe,
- COD measurement,
- High performance liquid chromatography (HPLC) and mass spectrometry (MS),
- Active species determination,
- Oxidizing agent.

2.5. Pilot design

- Pilot description and operating principles,
- Detail instructions,
- Timing program for Arduino circuit,
- Sedimentation procedure and catalyst recovery percentage.

2.6. Calculations

- Reaction rate constant and photochemical space-time yield (PSTY),
- Adsorption capacity,
- Flow rate for turbulent regime,
- Throughput for pilot plant.

Chapter 3. RESULTS AND DISCUSSION

3.1. Material characterizations

3.1.1. WS_2/g-C_3N_4 characterizations

3.1.1.1. X-ray diffraction patterns

Figure 3.1 shows the XRD patterns of 5WCN, 7WCN, 10WCN composites, WS_2, and g-C_3N_4. It can be observed from this figure that a high intensity diffraction peak at 27.4° and a weak one at 13.2° are characteristic of (002) and (100) planes of g-C_3N_4 respectively. For WS_2 sample, peaks at 13.6, 33.2 and 59.0° correspond to (002), (100) and (110) planes indexed to hexagonal phase of WS_2 (JPCDS card number 084–1398). The XRD patterns of the composites exhibit two peak systems corresponding to g-C_3N_4 and WS_2 phases.

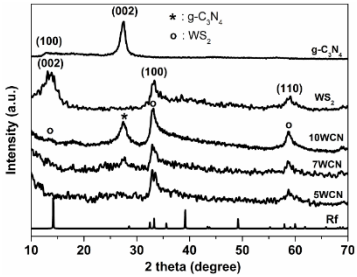

Figure 3.1. XRD patterns of 5WCN, 7WCN, 10WCN, WS_2, g-C_3N_4, and the reference for WS_2 (Rf).

3.1.1.7. X-ray photoelectron spectroscopy spectra

For the purpose of investigation the composition and chemical state of elements on surface of the composites, 10WCN was also analyzed by XPS spectra.

3.1.1.9. UV-Vis diffuse reflectance spectra

In order to evaluate the light-harvesting ability of the obtained samples, the UV-Vis diffuse reflectance spectra were conducted. As shown in Figure 3.10, g-C_3N_4 has an absorption edge at ~450 nm, which demonstrates the typical band gap of 2.7 eV for pure g-C_3N_4. WS_2 displays an extended absorption up to 800 nm due to the narrow band gap (~1.35 eV). For the composites, the absorption intensities strongly improved and extended to 800 nm, which can be explained by the contribution of optical absorption of WS_2. This extended optical absorption of the composites may result in an enhancement in photocatalytic activity under visible light.

In general, from the observed results prove that the synthesis of WS_2/g-C_3N_4 composite was successful using a facile method via heating the mixtures of tungstic acid and thiourea, in which thiourea was not only the source of S for forming WS_2 but also for the formation of g-C_3N_4 coating on the WS_2 nanosheets.

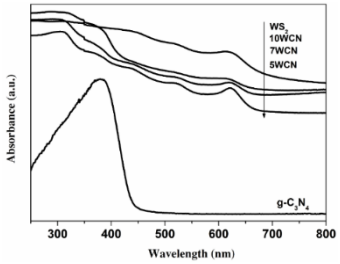

Figure 3.10. UV-Vis diffuse reflectance spectra of 5WCN, 7WCN, 10WCN composites, WS_2, and g-C_3N_4.

3.1.2. MoS_2/g-C_3N_4 photocatalyst

3.1.2.1. X-ray diffraction patterns

As indicated in Figure 3.11, the XRD patterns of g-C_3N_4 are observed as expected (JCPDS 87-1526). The two peaks located at 27.4º and 13º corresponds to the (002) stacking layered structure and the (100) in-plane repeated units, respectively, this is also consistent that of g-C_3N_4 in the previous section. The XRD pattern of MoS_2 could be ascribed to hexagonal phase (JCPDS 37-1492) with two peaks located at 32.6 ° and 58.3 ° corresponding to the (100) and (110), these planes are similar to that of WS_2 as mentioned above due to the same crystalline structure. The disappearance of interlayer (002) peak of MoS_2 indicates the formation of MoS_2 nanosheet. The XRD patterns for MCNx (x = 1, 2, 3, 5) are nearly the same as that for g-C_3N_4 and there is no recognizable diffraction peaks corresponding to MoS_2. This may be attributed to the low content of MoS_2 and its high dispersion in g-C_3N_4.

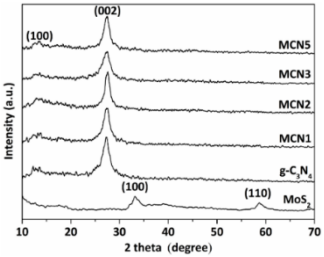

Figure 3.11. XRD patterns of MoS_2, g-C_3N_4, and MCNx (x = 1, 2, 3, 5).

3.1.2.3. X-ray photoelectron spectroscopy

The presence of MoS_2 in the composite samples can be confirmed by XPS, and MCN5 sample was chosen as a representative. As shown in Figure 3.13(a), the Mo 3d spectrum

exhibits two peaks at 228.0 eV (Mo $3d_{5/2}$) and 231.3 eV (Mo $3d_{3/2}$), and in Figure 3.13(b) the two peaks at 160.9 eV and 162.1 eV, correspond to the S $2p_{3/2}$ and S $2p_{1/2}$, respectively. This indicates the existence of Mo^{4+} and S^{2-} in the composite.

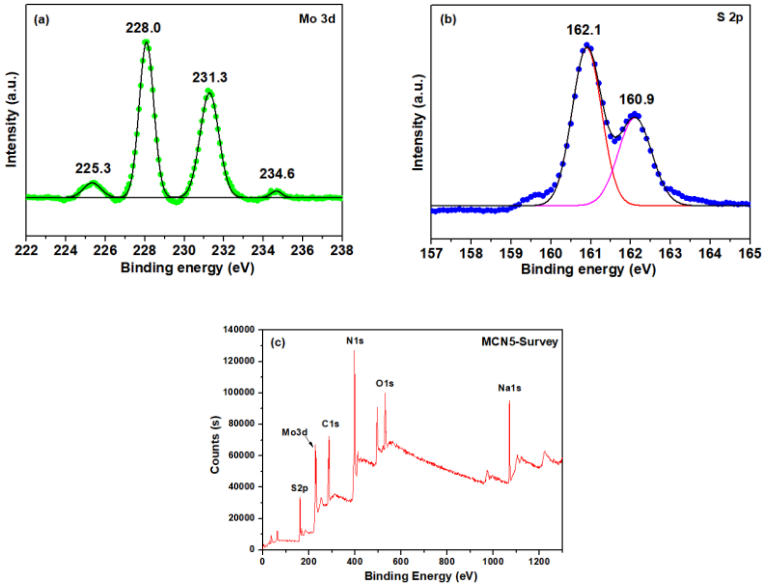

Figure 3.13. XPS spectra of Mo 3d (a), S 2p (b) and (c) XPS survey spectrum of MCN5 sample.

3.1.2.6. UV–vis diffuse reflectance spectroscopy

To investigate the light harvesting properties of the samples, UV–vis diffuse reflectance spectroscopy (DRS) was performed and the spectra are shown in Figure 3.16. The g-C_3N_4 sample shows absorption from UV through the visible range up to 450 nm which can be assigned to the intrinsic band gap of g-C_3N_4 (2.78 eV). For the composites, although there are not significant changes

in the band gap values (see detailed calculation in Figure 3.16b), the absorption intensity increases from MCN1 to MCN5 in the visible light region as compared to g-C_3N_4, which can be attributed to the presence of MoS_2 in the composite, resulting in high visible light photocatalytic performance. For MoS_2 sample, it could absorb light with the wavelength from 700 nm. The bandgap of MoS_2 nanosheet was 2.1 eV which calculated using Tauc plot method, this value is consistent with previous study.

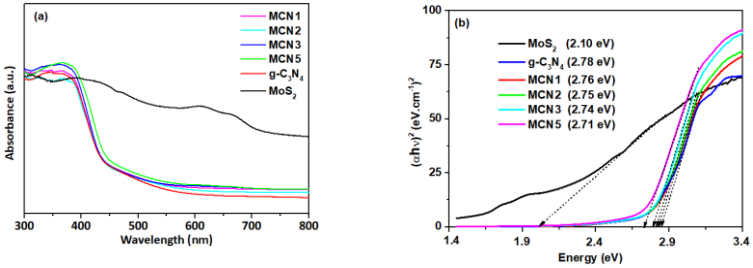

Figure 3.16. UV-Vis absorption spectra (a) and corresponding Tauc plots (b) of MoS_2, g-C_3N_4, and MCNx (x = 1, 2, 3, 5).

3.2. MATERIAL PHOTOCATALYTIC ACTIVITY

3.2.1. Adsorption-desorption equilibrium time

The needed time for reaching adsorption-desorption equilibrium of the material toward the target molecule is vital for the subsequent photocatalytic activity investigation.

3.2.2. Photocatalytic activity comparisons

The photocatalytic activity of all the WS_2/g-C_3N_4 samples was evaluated by methylene blue (MB) photodegradation in aqueous solution as shown in Figure 3.21. For comparison, the photocatalytic

activity of WS_2 and g-C_3N_4 are also presented. Figure 3.21 shows that WS_2 and g-C_3N_4 exhibited a low activity which may be due to high recombination rate of photogenerated electron-hole pairs in the pure semiconductors. For the composites, a strong improvement in activity can be observed from Figure 3.21 as well. However, their activities are different and can be graded in the order 10WCN < 5WCN < 7WCN, which indicates that among the as-prepared composites, the best photocatalyst is 7WCN with a MB degradation of 85.3% after 6 h under visible light irradiation. In order to clarify self-degradation of MB under visible light, a control experiment without photocatalyst was conducted. The result shows that the photolysis of MB can be ignored.

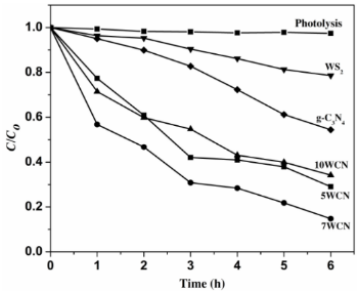

Figure 3.21. Photocatalytic degradation of MB on 5WCN, 7WCN, 10WCN, WS_2 and g-C_3N_4, and without photocatalyst. Conditions of process:irradiated volume: 90 mL, initial MB concentration: 30.0 mg.L^{-1}, pH 6.4, catalyst loading: 1.1 g.L^{-1}, 25°C, under 100 W incandescent lamp.

In order to investigate the best material of the MoS_2/g-C_3N_4 (MCNx) samples, their photocatalytic activities were evaluated by photodegradation of RhB, g-C_3N_4 also included for comparison.

As shown in Figure 3.23, there was an improvement in the photocatalytic activity of MCNx samples compared to the individual g-C_3N_4, except for MCN5 and this also indicates that the kinetic of the photodegradation processes were the pseudo-first-order, followed the Langmuir-Hinshelwood model. The composite MCN1 exhibited the best activity with the rate constant of 0.070 min^{-1}.

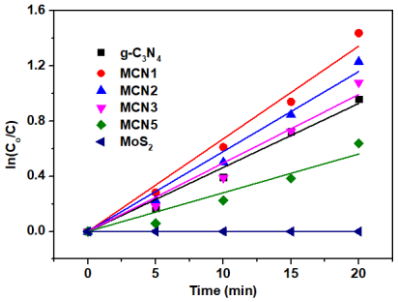

Figure 3.23. First-order kinetic plots for the photodegradation of RhB over MCNx and g-C_3N_4 samples. Conditions of process: irradiated volume: 25 mL, initial RhB concentration: 5.0 mg.L^{-1}, pH 3.0, catalyst loading: 0.7 g.L^{-1}, 25°C, under blue light. Except for MoS_2: initial RhB concentration: 25.0 mg.L^{-1}

3.2.3. Effect of catalyst loading

To find out the optimum catalyst dosage of MoS_2/g-C_3N_4, the photodegradation of RhB with various MCN1 loadings were carried out. When the catalyst loading increased from 0.3 g.L^{-1} to 0.7 g.L^{-1}, the RhB degradation rate increased due to an increase in the photogenerated electron-hole pairs. However, there is not a

significant change in the degradation rate when the catalyst loading is increased from 0.7 to 0.9 $g.L^{-1}$. Further increase in MCN1 loading results in a slight decrease in the RhB removal. This trend can be attributed to the negative effects of shielding by the suspended catalyst when the loading increased.

3.2.4. Adsorption and photocatalysis

3.2.4.1. Point of zero charge and existed forms of dye molecules

The experimental values of point of zero charge (pH_{pzc}) of MCN1 and 7WCN samples as shown were 3.6 and 2.1, respectively.

3.2.4.2. Effect of pH solution, important role of adsorption step

The effect of pH on photodegradation of both RhB and MB over the two catalysts of MCN1 and 7WCN was investigated with wide range values, which were adjusted before irradiation. The first dye we are going to explore the effect over the catalysts is RhB. As shown in Figure 3.30 for MCN1 sample, without adjusting medium (pH = 6.4), very low removal of RhB was observed. Increasing this value to 12.0, the degradation kinetics further slowed down. Surprisingly, a reduction of solution pH to 3.0 led to a dramatic increase of the RhB photodegradation, however, a further pH decrease to 1.5 resulted in a negative effect.

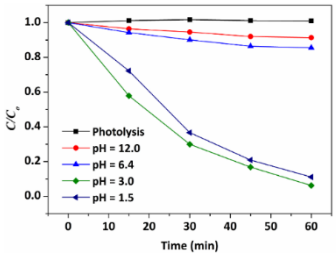

Figure 3.30. Effect of initial pH on RhB degradation over MCN1 photocatalyst. Process conditions: initial concentration, 5.0 ppm; catalyst loading: 0.7 g.L^{-1}; 25^{o}C; under blue light.

A pH-effect experiment on RhB degradation also was carried out over 7WCN catalyst as indicated in Figure 3.31. The trend is similar to that of RhB over MCN1, that means a low pH solution was favourable for the photodegradation reaction, however, this positive effect was interrupted if the solution was too acidic, at pH 1.5 as an example.

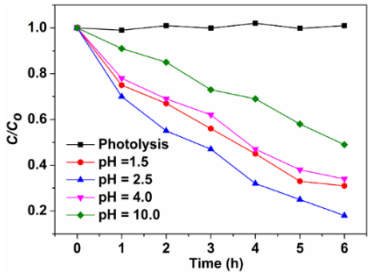

Figure 3.31. Effect of initial pH on RhB degradation over 7WCN photocatalyst. Process conditions: initial concentration, 30.0 ppm; catalyst loading: 1.1 g.L^{-1}; 25^{o}C; under 100 W incandescent lamp.

The specific amount of RhB adsorbed onto the catalysts was shown in Figure 3.32.

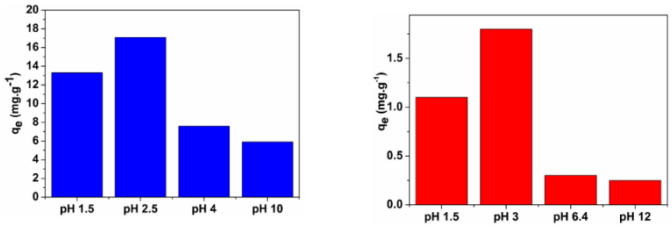

(a) (b)

Figure 3.32. Adsorption capacity of MCN1 (a) and 7WCN (b) materials toward RhB at different solution pHs

From the interestingly observed result about the effect of solution pH, thus the level of adsorbed target molecule onto the photocatalyst, on the photodecomposition rate we can come to conclusion that the adhere of the target to the surface of the catalyst during the photocatalytic process plays a vital role along with the different aspects such as the ability of that catalyst itself. No adsorption that means it is unlikely for the decomposition of the target due to the photocatalytic process to be happened, however, a too high adsorption capacity of the material towards the molecule might also cause possibly harmful effect to the photodegradation rate of that target.

3.2.5. A new benchmark for evaluation reaction reactor efficiency – Photochemical space time yield

3.2.5.1. Calculate reaction rate constant under optimal condition

Under optimal conditions as investigated in the previous section, the reaction rate constants for degrading RhB over 7WCN and MB over both MCN1 and 7WCN materials were calculated

using linear fit model. The rate constant for reaction of RhB over MCN1 was evaluated with the same method having the value of 0.070 min^{-1}.

These rate constants will be used to calculate the photochemical space-time yield (PSTY) of the relevant systems in the following sub-sections.

3.2.5.2. PSTY calculations for the chosen reaction systems

The calculated PSTY values for the two reaction systems that using the prepared catalysts MoS_2/g-C_3N_4 and WS_2/g-C_3N_4 indicates that each of dyes RhB and MB which was photodegraded over MoS_2/g-C_3N_4 has a much larger PSTY value than that of the corresponding one over WS_2/g-C_3N_4. Specifically, the PSTY values for degradation of RhB and MB over MoS_2/g-C_3N_4 are 3 and 2 order of magnitude larger than those of RhB and MB over WS_2/g-C_3N_4, respectively. The key reasons for this might come from not only the photocatalytic activity of the catalysts themselves, in which the adsorption capacities of the materials towards the dyes play a crucial role in the whole photocatalytic process as discussed in the previous section, but also come from how effective the used lamp converting electric energy into light form is and the spectrum of light produced from that lamp.

Because of the high PSTY value of MoS_2/g-C_3N_4 system, specifically MCN1 sample, compared to WS_2/g-C_3N_4 as discussed above, all the rest sections just used this kind of system for further investigations.

3.2.6. Mechanism investigation

3.2.6.1. Effect of oxidant concentration

This result shows that how important the presence of an acceptor electron or an oxidant is to the photocatalytic process. Therefore, in the case of without adding oxidizing reagent, the dissolved oxygen in the aqueous solution becomes vital for the photocatalytic reactions. This observation supported the concluded point that we have discussed so far about the adsorption competition of target molecules against the disscoled oxygen molecule onto the surface of the photocatalyst leading to a decrease in the photodegradation rate.

3.2.6.2. Reactive species trapping experiments and proposed photocatalytic mechanism

Generally, the reactive species which participate in the surface reaction during the photocatalytic process, including hole, superoxide radical anion, hydroxyl radical, and electron. To explore which of them having the most contribution to the photocatalytic process, the corresponding reactive species scavengers were employed in the reaction system that use MoS_2/g-C_3N_4 as a photocatalyst to degrade RhB. The changes in RhB photodegradation rate indicated that all the used scavengers had negative effects on the photocatalytic activity of the catalyst to different extents in order of TEOA > BQ > TBA > DMSO. The result also indicated that TEOA scavenger exhibited much stronger inhibition showing that hole was the dominant reactive species in the photodegradation process of RhB over MCN1 catalyst under studied conditions. The significant role of hole in the

photodegradation of the dye was clarified by a proposed mechanism of transformation of RhB to intermediates.

3.2.7. Applications

3.2.7.1. Photodegradation of a selected antibiotic, enrofloxacin

The aim of the next part of this section is to evaluate the extent in which the ENR antibiotic being mineralized by MoS_2/g-C_3N_4 under blue LEDs. As shown in Figure 3.45 the changes of COD and concentration of the ENR solution after 4 hours of illumination are completely different. A reduction in COD of the solution for 8 hours of irradiation was also presented to explore more about the mineralization degree.

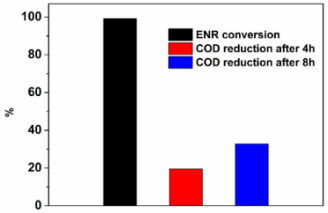

Figure 3.45. ENR conversion and COD reduction after 4 h of irradiation under LED blue light (0.2 A, 3.0 V), pH 4, initial concentration 5 ppm and volume of 20 mL, catalyst loading: 1 g.L^{-1}.

More specifically, while ENR in the solution was entirely degraded, its COD reduced only around 20% for the first 4 hours. This significant difference indicated that ENR itself could easily be totally degraded but not direct to simple molecules, instead it was partially oxidized to intermediates during the photocatalytic process.

3.2.7.2. Designed-pilot evaluation

To evaluate the throughput of the pilot RhB solution was used as simulated wastewater with the following conditions: 30 L of 5 ppm RhB solution at pH 3.5, MCN1 catalyst loading 0.7 $g.L^{-1}$, illuminated area 0.24 m^2 of 2 sets of blue LEDs (15 V, 5A), flow rate 8 $L.min^{-1}$. These conditions along with the distribution of wastewater as a thin layer which was previously proven good for the excitement of the catalyst also taken into account in the pilot design. Under these conditions, it took 120 h for that wastewater being completely treated, therefore the calculated pilot throughput was 1.0 $L.h^{-1}.m^{-2}$.

CONCLUSIONS

This thesis has achieved some accomplishments are as follows:

1. The heterojunction WS_2/g-C_3N_4 composites was successfully constructed via a facile calcination directly from the precursors of tungstic acid and thiourea in the solid state. Weight ratio of WS_2 to g-C_3N_4 in the composites affects their photocatalytic activities. Among the composites, 7WCN (synthesized from H_2WO_4 and thiourea with the mass ratio 1:7) is the best material which could photodegrade 85.3% MB in 6 hours under visible light. A synergistic effect of components in heterojunction of the composites for enhancing photocatalytic performance was proposed. In addition, the MoS_2/g-C_3N_4 composites were also synthesized by a simple method from sodium molybdate and thiourea in solid state, without the need for hydrothermal-condition and ultrasound process steps. The synthesized composites were proven to be efficient and active in photocatalysis, especially the MCN1 (synthesized from heating the mixture of 0.06 gram MoS_2 and 24.0 grams of thiourea under N_2 gas) sample with the optimum MoS_2 content in which the interfacial charge transfer increased and thus reduced electron-hole recombination, improving the photocatalytic activity.

2. The adsorption step plays a crucial role in the whole photocatalytic process, the more the target molecules adsorb on the photocatalyst's surface the faster they would be photodegraded. However, too many the adsorbed molecules on the surface could lead to a negative effect on the overall photodegradation rate due

to the lack of oxidizer on that surface such as oxygen. Furthermore, the mechanism of the transformation of target molecule such as rhodamine B to the intermediates such as rhodamine 110 was also proposed to provide a deep insight into the site of the molecule which was more likely to happen.

3. The reaction system used MoS_2/g-C_3N_4 photocatalyst and light-emitting diode (LED) was proven to have a value of new benchmark photochemical space-time yield (PSTY) of $8.3x10^{-3}$ $day^{-1}.kW^{-1}$, which was 100 times higher than that of the previous system also employed the same photocatalyst MoS_2/g-C_3N_4 over the same target molecule rhodamine B.

4. The designed photocatalytic pilot can operate automatically and use the prepared catalyst along with the application of natural sedimentation for recycling photocatalyst opens a new door to transfer the lab-scale into various practical applications including wastewater treatment under visible light.

LIST OF PUBLICATIONS

1. Huu Ha Tran, **Duy Huong Truong**, Thanh Tam Truong, Thi Xuan Dieu Nguyen, Ying-Shi Jin, Sung Jin Kim, and Vien Vo, "A Facile Synthesis of WS_2/g-C_3N_4 Composites with Improved Photocatalytic Activity," *Bull. Korean Chem. Soc.*, vol. 39, no. 8, pp. 965–971, 2018.

2. **D. H. Truong**, V. Vo, T. Van Gerven, and M. E. Leblebici, " A Facile Method for the Synthesis of a MoS_2 /g-C_3N_4 Photocatalyst ," *Chem. Eng. Technol.*, pp. 1–15, 2019.

3. Nguyễn Thị Thanh Bích, Nguyễn Đức Nhận, Huỳnh Hữu Điền, Nguyễn Tống Yến Như, Phạm Thị Yến Nhi, Nguyễn Văn Phúc, **Trương Duy Hướng**, Võ Viễn, "Effect of pH on Adsorption – Photocatalysis of Tunsten Disulfide", *Science Journal of Quy Nhon University*, 2020.

4. Trần Hữu Hà, Trần Doãn An, Nguyễn Văn Phúc, Nguyễn Thị Việt Nga, **Trương Duy Hướng**, Nguyễn Phi Hùng, Võ Viễn (2017), Tổng hợp và biến tính g-C_3N_4 bởi MS_2 (M = Mo, W) ứng dụng làm chất xúc tác quang, *Tạp chí Khoa học Trường Đại học Quy Nhơn*, tập 11, số 5/2017, tr 23-32.